Manuscript
Click here to download Manuscript: paper alumina para J Mat Sci - corregido (1).docx
Click here to view linked References

Hardness and flexural strength of single-walled carbon nanotube / alumina composites.

A. Gallardo-López [a,b,*], R. Poyato [b], A. Morales-Rodríguez [a,b], A. Fernández-Serrano [a], A. Muñoz [a,b], A. Domínguez-Rodríguez [a]

[a] *Departamento de Física de la Materia Condensada, Universidad de Sevilla, apdo. 1065, 41080 Sevilla, Spain*

[b] *Instituto de Ciencia de Materiales de Sevilla, CSIC-Universidad. de Sevilla, Avda. Américo Vespucio 49, 41092 Sevilla, Spain*

*e-mail: angela@us.es**

Phone numbers: +34 620612167, +34 954554448

Abstract

This work adds new experimental facts on room temperature hardness and flexural strength of alumina and composites with 1, 2, 5 and 10 vol.% single walled carbon nanotubes (SWNT) with similar grain size. Monolithic Al_2O_3 and composites were spark plasma sintered (SPS) in identical conditions at 1300ºC, achieving high density, submicrometric grain size and a reasonably homogeneous distribution of SWNTs along grain boundaries for all compositions with residual agglomerates. Vickers hardness values comparable to monolithic alumina were obtained for composites with low (1 vol.%) SWNT content, though they decreased for higher concentrations, attributed to the fact that SWNT constitute a softer phase. Three point bending flexural strength also decreased with increasing SWNT content. Correlation between experimental results and microstructural analysis by electron microscopy indicate that although SWNT agglomerates have often been blamed for detrimental effects on the mechanical

properties of these composites, they are not the main cause for the reported decay in flexural strength.

Keywords: Alumina; Carbon nanotubes; Nanocomposites; Flexural strength; Hardness.

1. Introduction

The extremely high tensile strength exhibited by carbon nanotubes (CNTs) [1], outstanding theoretical Young modulus and elevated resilience make them ideal candidates for reinforcement of brittle materials. Adding CNTs to a ceramic matrix can change not only mechanical properties, but also electrical and thermal conductivity [2-4]. Amongst structural advanced ceramics, alumina is most relevant due to its high resistance to corrosion, chemical stability and hardness [5]. CNTs retard grain growth in ceramic matrices and reduce sintering temperature, allowing fabrication of polycrystalline composites with refined microstructure [6]. Many properties as hardness, fracture toughness, wear, thermal shock resistance and superplasticity improve with grain size refinement [7-10]. Carbon nanotubes arrange themselves along grain boundaries, so they could also prevent crack propagation increasing fracture toughness by means of crack bridging, pull out, debundle and uncoiling of CNT ropes [11-13]. However, despite previous considerations and although some published results point to a reinforcement effect of CNT/Al_2O_3 composites, there is an ongoing controversy on this topic [4, 14-20]. One of the basic reasons for this is that composites have been widely compared to monolithic alumina differing in relevant microstructural features (mainly differences in grain size and in density-porosity of the samples) [21-26]. In most cases, these microstructural differences have not been quantified nor taken

into account, so a systematic comparison between monolithic alumina and composites starting from known similar microstructures is required to determine the role of CNTs.

The wide range of hardness and toughness values in CNT/Al_2O_3 composites reported in the literature has been mainly attributed to the inhomogeneous microstructure of the samples due to the CNT's tendency to agglomeration via Van der Waals forces. Several processing routes have been proposed to achieve homogeneous dispersion of the CNTs in the ceramic matrix, including acid treatments to the CNTs [27, 28], milling, and colloidal processing [4, 13, 26]. Spark plasma sintering (SPS) allows fabrication of fully dense composites with lower values of sintering temperature and applied pressure than conventional techniques. Sintering times are also considerably reduced due to the high heating rates, achieving a better control of grain size [29, 30] and minimizing damage to the CNTs [17, 31].

Another source of controversy in toughness values for CNT/Al_2O_3 composites arises from experimental difficulties. Vickers indentation (direct crack measurement, DCM) is a very questionable method for measuring fracture toughness in these materials, due to the systematic absence of radial cracks, more evident for high SWNT contents [31, 32]. This has been typically attributed to the redistribution of stresses under the indenter due to SWNTs [32] or to rough surface finish and porosity [31].

In this study, fabrication of fully dense Al_2O_3 and SWNT/Al_2O_3composites with 1, 2, 5 and 10 vol % SWNT has been addressed by colloidal processing and SPS, pursuing a dense homogeneous microstructure with submicrometric ceramic grains surrounded by disperse SWNTs at the grain boundaries. Microstructure of the sintered materials has

been characterized, as well as room-temperature hardness by Vickers indentation and flexural strength by three-point bending tests. Since both alumina and composites have been sintered with the same conditions and also exhibit similar grain size and density, the reinforcement capability of the SWNT can be clearly separated from their grain size refinement effect.

2. Experimental procedure

2.1. Materials processing

Purified SWNTs (Carbon Solutions Inc., Riverside, California, EEUU) were acid treated as detailed in [33]. α-alumina powder with 30-40 nm particle size and 99% purity (Nanostructured and Amorphous Materials Inc. Houston, Texas, EEUU) was used for the ceramic matrix. Colloidal processing by charge stabilization of the composite powders with different SWNT content (1, 2, 5 and 10 vol %) was carried out as described elsewhere [33].

SPS equipment Syntex Inc. Model 515S (Dr Sinter Inc, Kanagawa, Japan) was used to sinter the samples, with graphite molds. Sintering temperature and soaking time to obtain full density and grain size ≤ 1 μm were optimized for alumina in a preliminar study [34], and the optimized conditions were applied to the composites: 1300ºC, 5 minutes soaking time and 75 MPa applied pressure. Heating and cooling ramps were 300 ºC/min and 50 ºC/min, respectively. Density of sintered specimens (15 mm diameter x 2 mm thickness discs) was measured by Archimedes' method.

2.2. Microstructural characterization

Raman spectroscopy was used to confirm the presence of SWNTs and their integrity in the sintered specimens. A Raman spectrometer Horiba Jobin Yvon LabRam HR800 (Kyoto, Japan), with Olympus BX 41 optic and acquisition software LabSpec 5.25.15 was used. Qualitative characterization of the fracture surface of composites and grain morphology was carried out with high resolution scanning electron microscopy, (HRSEM HITACHI S5200, CITIUS facilities, Univ. of Sevilla). Top surfaces and cross sections of the sintered alumina and composite disks were polished and thermally etched in air. Grain size was characterized by the equivalent planar diameter of 300 grains, $d=2(area/\pi)^{1/2}$. Shape factor, $f = 4\pi\ area/perimeter^2$ and the degree of orientation were also estimated. The degree of orientation is defined by the orientation descriptor $f_p = [2<\cos^2(\varphi)> - 1]$ [35], or angle distribution function of the grains major axis with respect to average major axis ($\varphi = 0$). Therefore $f_p=0$ for random orientation and 1 for all grains aligned.

2.3. Mechanical tests

2.3.1 Hardness

Vickers indentation was performed at room temperature on sintered alumina and composites top surfaces polished to 1 µm diamond paste. Loads up to 2 kgf were applied by a Struers Duramin indenter. 30 imprints on each specimen (with enough spatial resolution to avoid interaction between deformed areas and fracture systems) were analyzed with a LEICA DCM 3D microscope. Vickers hardness, H_v, was estimated from the applied load P, and the imprint's diagonal d : $H_v = 1.8544\frac{P}{d^2}$.

2.3.2. Flexural Resistance

In order to test the flexural resistance of sintered alumina and composites (15 mm discs), a special three-point bending test assembly with 10 mm span was designed to adapt to the small size of the samples. This assembly was attached to a universal INSTRON machine 1165. The tests were performed at a speed of 0.5 mm/min at room temperature. Samples of 15x2x1 mm^3 size were cut from SPSed discs and one surface was polished to 1 µm. Only composites with lower SWNT contents (1 and 2 vol % SWNT) were successfully prepared; the extreme fragility of the others resulted in catastrophic failure during the process.

3. Results and discussion

3.1. Microstructural characterization

Composites with 1, 2, 5 and 10 vol % SWNT showed an improved densification with increasing SWNT content (Table 1). Figure 1 displays typical sintering shrinkage curves from SPS for different composites showing that increasing SWNT content seems to advance densification start. This is consistent with the fact that higher SWNT contents make the powders more conductive, thus achieving higher local temperatures [16]. Some authors have found that sintering temperature to achieve full density of MWNT/Al_2O_3/composites decreases 500ºC compared to pure alumina due to the improved self-lubricating properties of SWNTs, which promote compactibility and compressibility of the nanocomposites powder [6].

Raman spectra of the composites reveal the presence of SWNT characteristic bands, in particular the low frequency radial breathing mode (RBM) and the G band (spectra shown in figure 2), confirming absence of significant damage to the SWNTs during processing and sintering. D band, associated to crystalline defects is also observed. ID/IG ratio has also been calculated, showing an increasing trend with increasing

SWNT content (14, 14, 28 and 42% for 1, 2, 5 and 10 vol% respectively), which indicates a larger amount of crystalline defects in the nanotubes. This agrees with the mentioned hypothesis about current-induced damage to the SWNT during SPS or their carbothermal reduction, which would both increase with higher SWNT content.

HRSEM images (figure 3) show the typical appearance of the composite fracture surfaces with well dispersed SWNT for all the compositions although some agglomerates (fig. 3d) are also present. In all cases SWNTs are located at grain boundaries, covering partially the ceramic grains. They show a blanket-like aspect, like a dark layer. A similar feature has also been observed by several authors in SWNT/Al_2O_3 composites [32, 36, 37]. For MWNT/Al_2O_3 composites only Huang *et al.* [38] observed this particular microstructure in a fracture surface. It has been attributed to carbon diffusion into the alumina matrix grains, due to a high-current-induced damage on carbon nanotubes during SPS [16] and to an Al_2OC layer between the SWNTs and the alumina grains formed by a carbothermal reduction [24]. Increasing SWNT concentration results in an extended SWNT layer, covering a greater area of ceramic grains, as it can be seen in figure 3 comparing composites with low SWNT content (a) and (e) with higher SWNT content (c) and (f). This should have a direct influence on the mechanical properties of the composites. More details about the microstructure are given in a previous study [39].

Microstructural data for monolithic alumina are shown in table 1. Anomalous grain growth has been detected, with maximum grain sizes $d_{max} > 5d$ (not shown), a characteristic feature of alumina [34]. Slight alignment of elongated grains has been determined with a preferential grain orientation factor of 0.3 for monolithic alumina, probably due to uniaxial applied pressure during SPS. Composites exhibit a very slight

grain refinement for the higher SWNT content and also show a more homogeneous grain size distribution, since the standard deviation of their mean grain size decreases to half its value relative to monolithic alumina. This refinement is indicative of homogeneous SWNT distribution, good dispersion and survival of SWNTs, since grain growth retardation is produced by the SWNT when effectively dispersed along grain boundaries (GBs) [40]. SWNT at ceramic GBs partially block and impede both grain boundary sliding and diffusion during densification at high temperature, inhibiting grain growth kinetics during sintering. Therefore, the higher surface fraction of Al_2O_3 grains in contact with SWNTs the lower the grain size after sintering [41]. However, the grain refinement effect of SWNTs depends also highly on the sintering temperature [6], being greater with increasing temperature. At 1300ºC, sintering temperature of samples in this study, the effect of the various SWNTs contents is roughly the same. The ceramic grains tendency to align perpendicularly to applied pressure during sintering is more remarkable in composites than in monolithic alumina (in fact the orientation factor is double for composites with 1 vol% SWNT), although if we focus only in the composites, the orientation factor diminishes with increasing SWNT content. The lubricant effect of the SWNTs [40] would facilitate grain rotation during sintering in composites and alignment of the grains along a preferential axis. When SWNT content increases, however, the lubricant effect of a small amount of well dispersed nanotubes (also invoked to explain higher densification rate [6]) would be counterbalanced by the tendency of SWNTs to entangle and dispose randomly in the grain boundaries. Increasing the size of the SWNT layer would act then as an obstacle to grain rearrangement with pressure, in addition to constraining grain growth and would also influence the high temperature mechanical properties. This is in agreement with the results of Zapata *et al.* [42], who found a large decrease in the creep rate of 10 vol%

SWNT/Al_2O_3 composites tested at 1300 and 1350ºC. These authors claim that SWNTs partially inhibit diffusion along grain boundaries and block grain boundary sliding, although marginal grains may still slide. Apart from these slight effects of SWNT addition on grain size, densification and grain arrangement of the composites, the similarity of microstructural parameters to those of monolithic alumina allow us to compare their mechanical properties and evaluate the influence of the SWNTs in the alumina matrix unambiguously.

3.2. Mechanical properties.

3.2.1 Vickers hardness

There is not any increase nor decrease of hardness within the experimental error for composites with 1 vol % SWNT with respect to monolithic alumina. A 25% decrease in hardness is found for composites with higher SWNT content (3, 5 and 10 vol %), see figure 4. Correct measurement of the imprints' diagonal became more difficult with increasing SWNT content, producing a greater dispersion of the results and diminishing their reliability. Values of hardness obtained for monolithic alumina and composites are similar to other authors [31, 32] (figure 4). Feasible reasons for decrease of hardness with higher SWNT content considered in the literature are the presence of soft phases at the alumina grain boundaries, poor adherence CNT-ceramic grain, graphitic (lubricant) nature of CNTs and poor dispersion of CNTs in the alumina matrix (agglomerates), which could cancel out the improvement of the room temperature mechanical properties achieved by the grain refinement [23, 25, 26, 43, 44]. Our results indicate that the decrease in hardness with SWNT content is rather due to the fact that CNTs located at the GBs are a softer phase than the alumina ceramic matrix (hardness of MWNT in

radial direction is 6-10 GPa at GBs [44]). SWNT accumulation at grain boundaries is also likely to deteriorate their interfacial cohesion with the ceramic matrix [26].

3.2.2. Flexural strength

Results of flexural strength of monolithic alumina and composites with 1 and 2 vol % SWNT are presented in table 2, showing a clear decrease of flexural strength versus carbon nanotube content. We should remark the very little dispersion of the results for each composition, which demonstrates the homogeneity of the tested materials. These flexural strength values are higher and not directly comparable to values in the literature for similar materials, since the experimental set up was designed out of the ASTM standard C1161 [45]. A higher flexural strength is expected due to the smaller size of the specimens. However, our results are valid to compare the different compositions tested in this study and therefore to evaluate the effect of SWNTs in the alumina matrix. Only Liu *et al.* [43] used the same experimental conditions (same specimen dimensions) for SPS dense monolithic alumina. We obtain a much higher value of flexural strength, most likely due to our smaller average grain size (0.6 versus 1.9 μm). Figure 5 shows a linear decrease in flexure resistance of alumina composites with increasing SWNT content. Although absolute values are not significant, the flexure strength behavior can be compared to other authors' who used standard experimental settings. MWNT /Al_2O_3 composites are included in the comparison due to the scarce results found in the literature for flexural strength in alumina composites with SWNT. Fan *et al.* [21] (SWNTs) and Kim *et al.* [22] (MWNTs) found an opposite trend for low CNT concentration, conventionally sintered composites, with flexure strength increasing with SWNT content, see figure 5. The explanation for this apparently contradictory behavior

has to take into account that flexure strength is strongly affected by grain size. The CNT refinement effect on the matrix grains is greater at higher temperatures, such as those reached in conventional sintering by the previous authors (1550ºC-1600ºC) though no microstructural parameters were indicated in the mentioned studies. Therefore, an increase in flexural strength when adding CNTs is expected due to a significant grain refinement. For a critical amount of CNTs (1-1.5 vol%), the grain growth inhibiting effect is counterbalanced by their softening effect, and flexure strength decreases. Only a recent work with double-wall carbon nanotubes (DWNT) / alumina composites [46] reports a slight increase in flexure strength with higher CNT content -4,4 vol% DWNT- with respect to monolithic alumina. These authors also found an increase in the composite fracture toughness due to crack bridging by non-functionalized DWNTs. Yamamoto *et al.* [23] found a simultaneous increase of fracture toughness and bending strength with the addition of a small amount (1 vol%) of large diameter MWCNTs in SPS composites with respect to monolithic alumina, and a further degradation of mechanical properties for increasing MWCNTs content (2, 4 and 7 vol%). The improvement was attributed to a high structural homogeneity and enhanced frictional resistance of the structural components, while degradation was attributed primarily to severe phase segregation, giving CNTs aggregates a similar role to pores in the matrix. However, the high sintering temperatures used by these authors (1500ºC) make us think that the increase of bending strength in the composites relative to monolithic alumina may be due to the pronounced refinement effect of the CNTs on the alumina grains, (mentioned in the paper but not quantified), since a great difference in CNT aggregation is not likely to occur when changing from 1 to 2 vol%. The trend for the composites (decreasing bending strength with increasing CNT content) is then the same as in our work. Other authors [25, 26, 47] with poor densification of their Al_2O_3/CNT composites

have reported elongated pores that could be responsible for lower flexural strength, but we have not observed any pores.

Poorteman *et al.* [48] correlate the presence of dark zones at or near the fracture origin with the presence of nanotube agglomerates. If we assume, as proposed in the literature [21, 23, 25, 37] that SWNTs agglomerates are the critical flaws for fracture in the studied composites, a rough estimation of fracture toughness K_{IC}, could be made. Using the Griffith Equation and assuming a small half-penny crack stressed in an opening mode: $K_{IC} = 1.12\left(\frac{2\sigma_y}{\pi}\right)\sqrt{\pi a_c}$. Taking experimental values of the flexural strength σ_y for composites with 1 and 2 vol% SWNT (see table 2) and assuming for the critical flaw size a_c the maximum size of SWNT agglomerates determined by SEM for each composition, (~40 μm for both cases, similar to estimations of 50 μm by [37] in 0.6 vol% MWNTs) we obtain values of K_{IC} of 4.6 and 2.9 MPa $m^{1/2}$ respectively. It is remarkable that although the agglomerate maximum size does not change with SWNT content (not even the average size, ~6 μm for both composites), the flexural strength decreases considerably. This would rule out the SWNT agglomerates as the main cause of fragility of these SWNT/Al_2O_3 composites, opposite to what has been often proposed in the literature [21, 23, 25, 37, 48]. Instead, this supports the idea of SWNTs weakening interfacial cohesion between alumina grains. As the SWNT content increases, the fraction of alumina grains covered by the SWNT "blanket" also increases, resulting in decreasing toughness and strength. Although our three point bending experiments give for monolithic alumina higher values of flexural strength than standard tests [22, 23, 43] for the reasons mentioned before, values for composites are not so different [21, 22, 37], in spite of the smaller dimensions of specimens and refined grain size, which should increase flexural strength. This could be explained by the fact that smaller alumina grains can be more easily surrounded by the SWNTs, so if we

assume that the nanotubes weaken the interfacial cohesion between ceramic grains, lower flexural strength would be expected for composites.

4. Conclusions

1, 2, 5 and 10% vol SWNT/Al_2O_3 composites sintered by SPS at 1300ºC showed homogeneous microstructure with disperse SWNT at grain boundaries and few agglomerates. SWNT addition caused increased density, very slight grain refinement and slight increase in alignment of ceramic grains perpendicular to SPS pressure axis in composites. This enhanced re-arrangement effect decreases for high SWNTs content, probably due to entangling and random disposition of the SWNTs.

Vickers hardness for 1 vol% SWNT composites was similar to alumina, but decreased for higher SWNT contents, reaching a 25% diminution. This decrease is attributed to the fact that SWNTs located at the GBs are a softer phase than the alumina matrix.

Flexural strength of SWNT/Al_2O_3 also showed a remarkable decrease with SWNT content. This result linked to the fact that maximum and average SWNT agglomerate size does not change with SWNT content rules out these agglomerates as the main cause for the decrease in fracture toughness of the composites.

Acknowledgements

This work was financed by Spanish Ministry of Science and Innovation (MAT2009-11078 and MAT2012-34217) and by Junta de Andalucía (P12-FQM-1079). Microscopy studies were performed in CITIUS facilities (Universidad de Sevilla).

References

1. Li F, Cheng H, Bai S, Su G, Dresselhaus M (2000). Tensile strength of single-walled carbon nanotubes directly measured from their macroscopic ropes. Appl Phys Lett 77(20):3161-3163.

2. Inam F, Yan H, Jayaseelan DD, Peijs T, Reece MJ (2010). Electrically conductive alumina-carbon nanocomposites prepared by Spark Plasma Sintering. J Eur Ceram Soc 30(2):153-157.

3. Sivakumar R, Guo S, Nishimura T, Kagawa Y (2007). Thermal conductivity in multi-wall carbon nanotube/silica-based nanocomposites. Scr Mater 56(4):265-268.

4. Zhan GD, Kuntz JD, Wan JL, Mukherjee AK (2003). Single-wall carbon nanotubes as attractive toughening agents in alumina-based nanocomposites. Nature Materials 2(1):38-42.

5. Okada A (2008). Automotive and industrial applications of structural ceramics in Japan. J Eur Ceram Soc 28(5):1097-1104.

6. Inam F, Yan H, Peijs T, Reece MJ (2010). The sintering and grain growth behaviour of ceramic-carbon nanotube nanocomposites. Composites Sci Technol 70(6):947-952.

7. Xu H, Jahanmir S (1995). Effect of Grain-Size on Scratch Damage and Hardness of Alumina. J Mater Sci Lett 14(10):736-739.

8. Miyahara N, Yamaishi K, Mutoh Y, Uematsu K, Inoue M (1994). Effect of Grain-Size on Strength and Fracture-Toughness in Alumina. Jsme International Journal Series A-Mechanics and Material Engineering 37(3):231-237.

9. You X, Si T, Liu N, Ren P, Xu Y, Feng J (2005). Effect of grain size on thermal shock resistance of Al2O3-TiC ceramics. Ceram Int 31(1):33-38.

10. Hiraga K, Kim B, Morita K, Yoshida H, Suzuki TS, Sakka Y (2007). High-strain-rate superplasticity in oxide ceramics. Sci Technol Adv Mater 8(7-8):578-587.

11. Xia Z, Riester L, Curtin WA, Li H, Sheldon BW, Liang J, Chang B, Xu JM (2004). Direct observation of toughening mechanisms in carbon nanotube ceramic matrix composites. Acta Mater 52(4):931-944.

12. Mukhopadhyay A, Chu BTT, Green MLH, Todd RI (2010). Understanding the mechanical reinforcement of uniformly dispersed multiwalled carbon nanotubes in alumino-borosilicate glass ceramic. Acta Mater 58(7):2685-2697.

13. Padture NP (2009). Multifunctional composites of ceramics and single-walled carbon nanotubes. Adv Mater 21(17):1767-1770.

14. Sun J, Gao L, Iwasa M, Nakayama T, Niihara K (2005). Failure investigation of carbon nanotube/3Y-TZP nanocomposites. Ceram Int 31(8):1131-1134.

15. Laurent C, Peigney A, Dumortier O, Rousset A (1998). Carbon nanotubes Fe alumina nanocomposites. Part II: Microstructure and mechanical properties of the hot-pressed composites. J Eur Ceram Soc 18(14):2005-2013.

16. Thomson KE, Jiang D, Ritchie RO, Mukherjee AK. A preservation study of carbon nanotubes in alumina-based nanocomposites via Raman spectroscopy and nuclear magnetic resonance (2007). Appl Phys A-Mat Sci Proc 89(3):651-654.

17. Jiang D, Thomson K, Kuntz JD, Ager JW, Mukherjee AK (2007). Effect of sintering temperature on a single-wall carbon nanotube-toughened alumina-based nanocomposite. Scr Mater 56(11):959-962.

18. Ahmad K, Pan W (2008). Hybrid nanocomposites: A new route towards tougher alumina ceramics. Composites Sci Technol 68(6):1321-1327.

19. Mo C, Cha S, Kim K, Lee K, Hong S (2005). Fabrication of carbon nanotube reinforced alumina matrix nanocomposite by sol-gel process. Mat Sci Eng A-Struct 395(1-2):124-128.

20. Cha S, Kim K, Lee K, Mo C, Hong S (2005). Strengthening and toughening of carbon nanotube reinforced alumina nanocomposite fabricated by molecular level mixing process. Scr Mater 53(7):793-797.

21. Fan JP, Zhao DQ, Wu MS, Xu ZN, Song J (2006). Preparation and microstructure of multi-wall carbon nanotubes-toughened Al_2O_3 composite. J Am Ceram Soc 89(2):750-753.

22. Kim SW, Chung WS, Sohn K, Son C, Lee S (2009). Improvement of flexure strength and fracture toughness in alumina matrix composites reinforced with carbon nanotubes. Mat Sci Eng A-Struct 517(1-2):293-299.

23. Yamamoto G, Hashida T (2012). Carbon Nanotube Reinforced Alumina Composite Materials. In: Hu N, editor. Composites and Their Properties: InTech.

24. Ahmad I, Unwin M, Cao H, Chen H, Zhao H, Kennedy A, Zhu YQ (2010). Multi-walled carbon nanotubes reinforced Al2O3 nanocomposites: Mechanical properties and interfacial investigations. Composites Sci Technol 70(8):1199-1206.

25. Bakhsh N, Khalid FA, Hakeem AS. Synthesis and characterization of pressureless sintered carbon nanotube reinforced alumina nanocomposites (2013). Mat Sci Eng A-Struct 578:422-429.

26. Ahmad I, Cao H, Chen H, Zhao H, Kennedy A, Zhu YQ (2010). Carbon nanotube toughened aluminium oxide nanocomposite. J Eur Ceram Soc 30(4):865-873.

27. Liu J, Rinzler A, Dai H, Hafner J, Bradley R, Boul P, Lu A, Iverson T, Shelimov K, Huffman C, Rodriguez-Macias F, Shon Y, Lee T, Colbert D, Smalley R (1998). Fullerene pipes. Science 280 (5367):1253-1256.

28. Poyato R, Vasiliev AL, Padture NP, Tanaka H, Nishimura T (2006). Aqueous colloidal processing of single-wall carbon nanotubes and their composites with ceramics. Nanotechnology 17(6):1770-1777.

29. Omori M (2000). Sintering, consolidation, reaction and crystal growth by the spark plasma system (SPS). Mat Sci Eng A-Struct 287(2):183-188.

30. Munir ZA, Anselmi-Tamburini U, Ohyanagi M (2006). The effect of electric field and pressure on the synthesis and consolidation of materials: A review of the spark plasma sintering method. J Mater Sci 41(3):763-777.

31. Thomson KE, Jiang D, Yao W, Ritchie RO, Mukherjee AK (2012). Characterization and mechanical testing of alumina-based nanocomposites reinforced with niobium and/or carbon nanotubes fabricated by spark plasma sintering. Acta Mater 60(2):622-632.

32. Wang XT, Padture NP, Tanaka H (2004). Contact-damage-resistant ceramic/single-wall carbon nanotubes and ceramic/graphite composites. Nature Mater 3(8):539-544.

33. Poyato R, Gallardo-López A, Gutiérrez-Mora F, Morales-Rodríguez A, Muñoz A, Domínguez-Rodríguez A (2014). Effect of high SWNT content on the room temperature mechanical properties of fully dense 3YTZP/SWNT composites. J Eur Ceram Soc 34(6):1571-1579.

34. Morales-Rodriguez A, Poyato R, Gallardo-Lopez A, Munoz A, Dominguez-Rodriguez A (2013). Evidence of nanograin cluster coalescence in spark plasma sintered alpha-Al_2O_3. Scr Mater 69(7):529-532.

35. González L, Cumbrera F, Sánchez-Bajo F, Pajares A (1994). Measurement of Fiber Orientation in Short-Fiber Composites. Acta Metall Mater 42(3):689-694.

36. Vasiliev AL, Poyato R, Padture NP (2007);. Single-wall carbon nanotubes at ceramic grain boundaries. Scr Mater 56(6):461-463.

37. Poorteman M, Traianidis M, Bister G, Cambier F (2009). Colloidal processing, hot pressing and characterisation of electroconductive MWCNT-alumina composites with compositions near the percolation threshold. J Eur Ceram Soc 29(4):669-675.

38. Huang Q, Jiang D, Ovid'ko IA, Mukherjee A (2010). High-current-induced damage on carbon nanotubes: The case during spark plasma sintering. Scr Mater 63(12):1181-1184.

39. Morales-Rodríguez A, Gallardo-López A, Fernández-Serrano A, Poyato R, Muñoz A, Domínguez-Rodríguez A (2014). Improvement of Vickers hardness measurement on SWNT/Al2O3 composites consolidated by spark plasma sintering. J Eur Ceram Soc. In press, DOI: 10.1016/j.jeurceramsoc.2014.05.048.

40. Peigney A, Flahaut E, Laurent C, Chastel F, Rousset A (2002). Aligned carbon nanotubes in ceramic-matrix nanocomposites prepared by high-temperature extrusion. Chem Phys Lett 352(1-2):20-25.

41. Zapata-Solvas E, Gomez-Garcia D, Dominguez-Rodriguez A (2012). Towards physical properties tailoring of carbon nanotubes-reinforced ceramic matrix composites. J Eur Ceram Soc 32(12):3001-3020.

42. Zapata-Solvas E, Gómez-García D, Domínguez-Rodríguez A (2010). On the microstructure of single wall carbon nanotubes reinforced ceramic matrix composites. J Mater Sci 45(9):2258-2263.

43. Liu L, Hou Z, Zhang B, Ye F, Zhang Z, Zhou Y (2013). A new heating route of spark plasma sintering and its effect on alumina ceramic densification. Mat Sci Eng A-Struct 559:462-466.

44. Inam F, Peijs T, Reece MJ (2011). The production of advanced fine-grained alumina by carbon nanotube addition. J Eur Ceram Soc 31(15):2853-2859.

45. ASTM C1161 - 13, (1996) Standard Test Method for Flexural Strength of Advanced Ceramics at Ambient Temperature. In: Anonymous Book of Standards, vol. 15.01.

46. Kasperski A, Wibel A, Estournès C, Laurent Ch, Peigney A (2013). Preparation-microstructure-property relationships in double-walled carbon nanotubes/alumina composites. Carbon 53: 62-72.

47. Flahaut E, Peigney A, Laurent C, Marliere C, Chastel F, Rousset A (2000). Carbon nanotube-metal-oxide nanocomposites: Microstructure, electrical conductivity and mechanical properties. Acta Mater 48(14):3803-3812.

48. Poorteman M, Descamps P, Cambier F, Leriche A, Thierry B (1993). Hot Isostatic Pressing of SiC-Platelets Y-Tzp Composites. J Eur Ceram Soc 12(2):103-109.

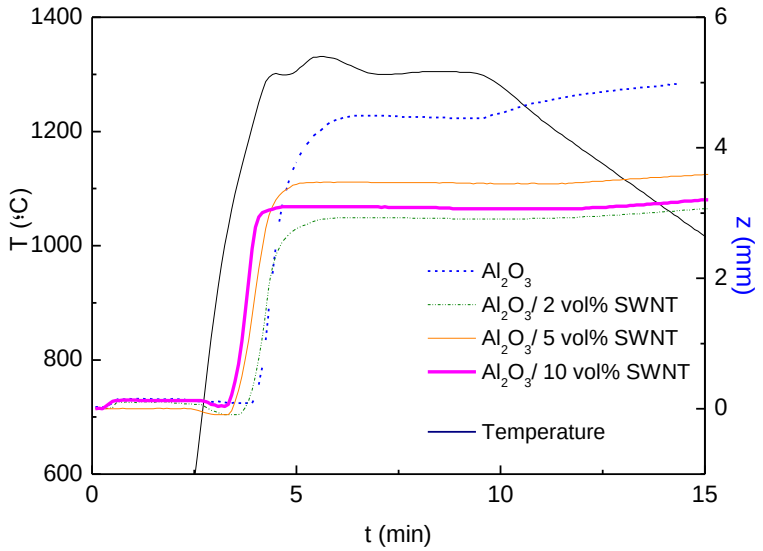

Fig. 1 Temperature and densification curve (z) versus time for Al_2O_3 and SWNT/Al_2O_3 composites sintered at 1300ºC, for 5 min, and 75 MPa

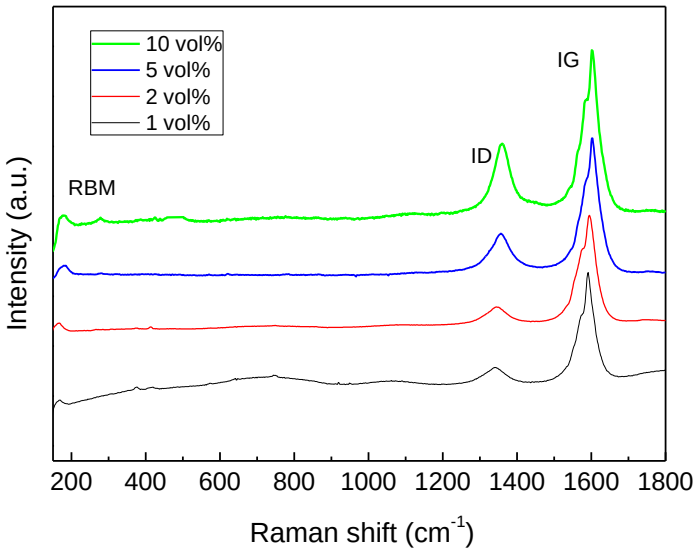

Fig. 2 Raman spectra corresponding to the different SWNT/Al_2O_3 composites sintered in this work.

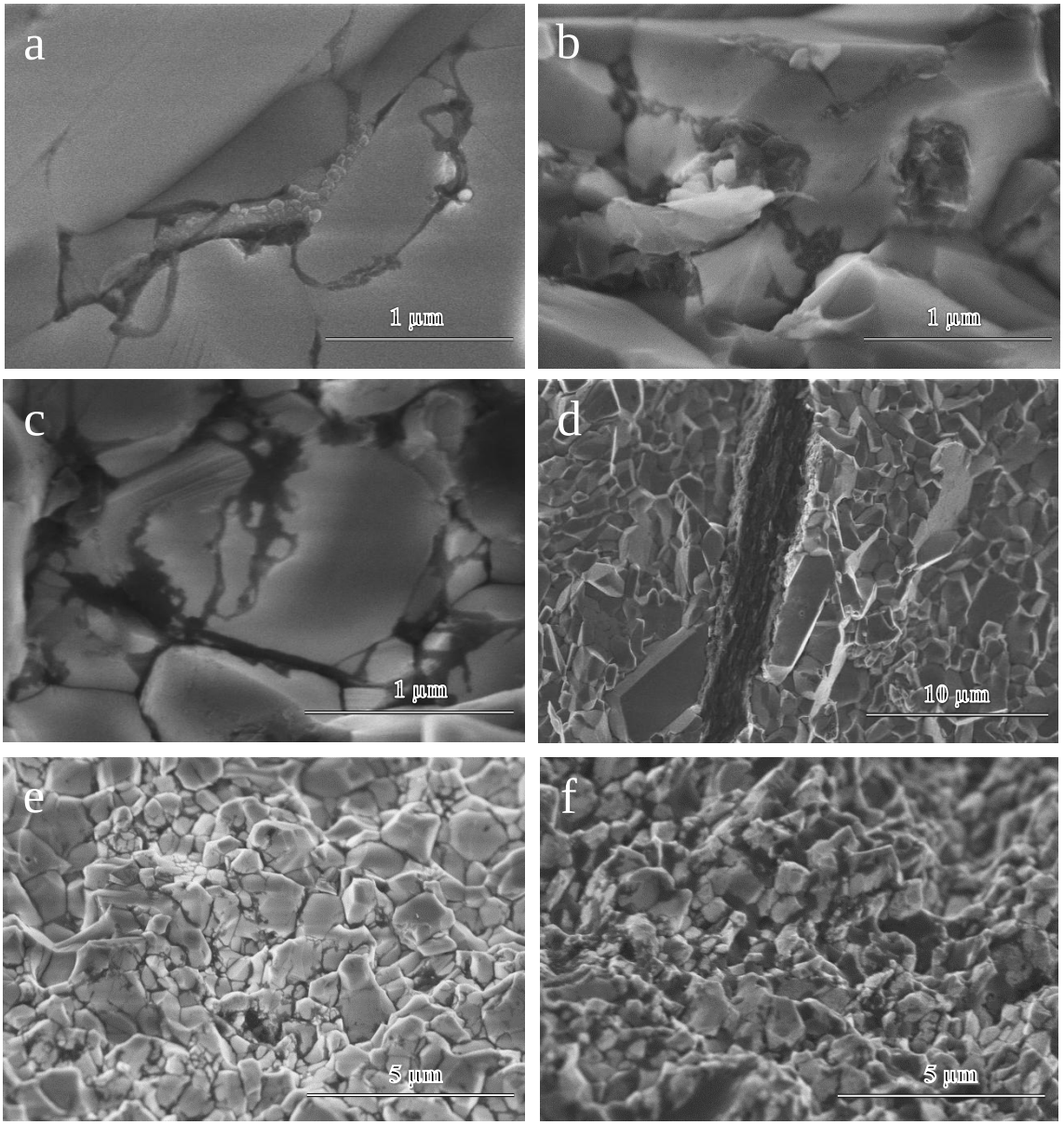

Fig. 3 HRSEM micrographs of typical SWNT/Al_2O_3 composite fracture surfaces: a) 1 vol % SWNT, b) 5 vol % SWNT, c) 10 vol% SWNT, d) SWNT agglomerate in 5 vol % SWNT, and low magnification e) 2 vol% SWNT and f) 10 vol% SWNT.

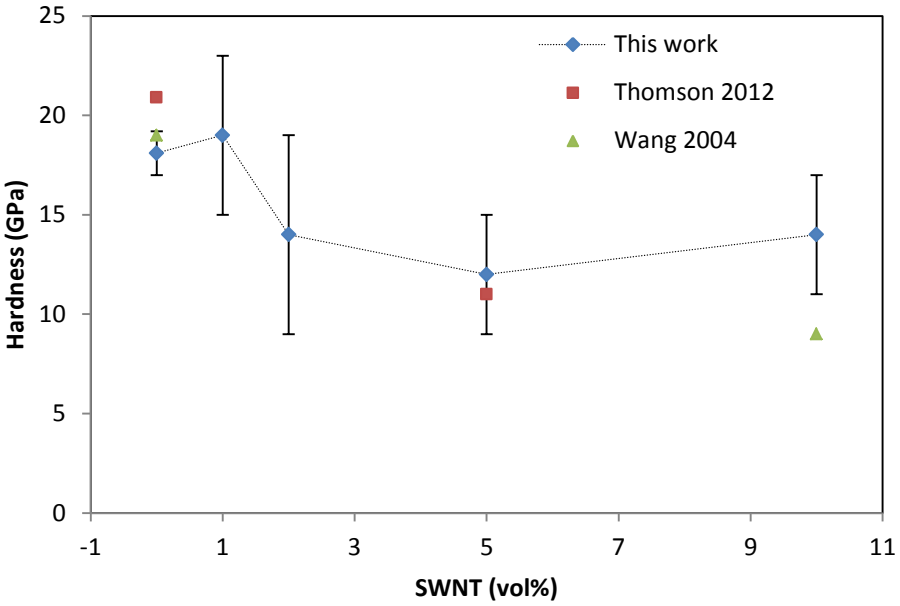

Fig. 4 Hardness versus SWNT content for Al_2O_3 and SWNT/Al_2O_3 composites [31, 32]

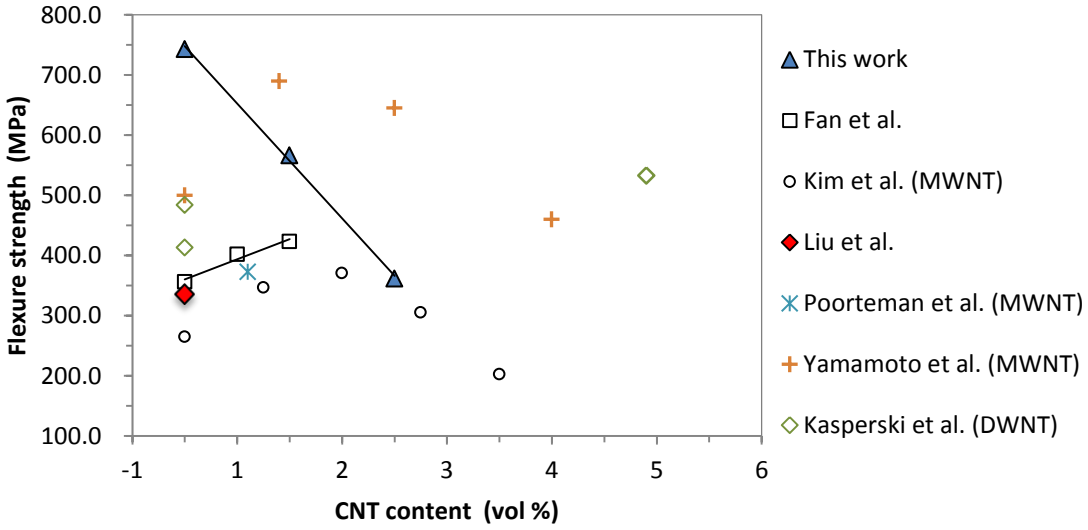

Fig. 5 Flexural strength of Al_2O_3 and SWNT/Al_2O_3 composites versus CNT content and comparison with the literature [21-23, 27, 43, 46, 48]

Table 1 Density and microstructural parameters for Al_2O_3 and SWNT/Al_2O_3 composites.

SWNT vol %	**Relative density (%)**	**d (µm)**	**sd (µm)**	**Shape factor, F**	**Preferential orientation [f_p= 0 – 1]**
0	98.4	0.7	0.6	0.67 ± 0.14	0.3
1	98.5	0.6	0.4	0.68 ± 0.10	0.5
2	99.4	0.7	0.4	0.67 ± 0.12	0.4
5	99.8	0.5	0.4	0.71 ± 0.17	0.4
10	100.0	0.5	0.3	0.72 ± 0.16	0.3

Table 2. Flexural strength measured for each tested sample and average values.

SWNT (Vol %)	**σ_f (MPa)**	**$<\sigma_f>$(MPa)**
0	770 ± 9	740 ± 50
	740 ± 8	
	680 ± 8	
	780 ± 9	
1	570 ± 6	570 ± 50
	610 ± 7	
	520 ± 6	
2	330 ± 4	360 ± 40
	400 ± 4	

Figure 1
Click here to download Figure: Fig1.eps

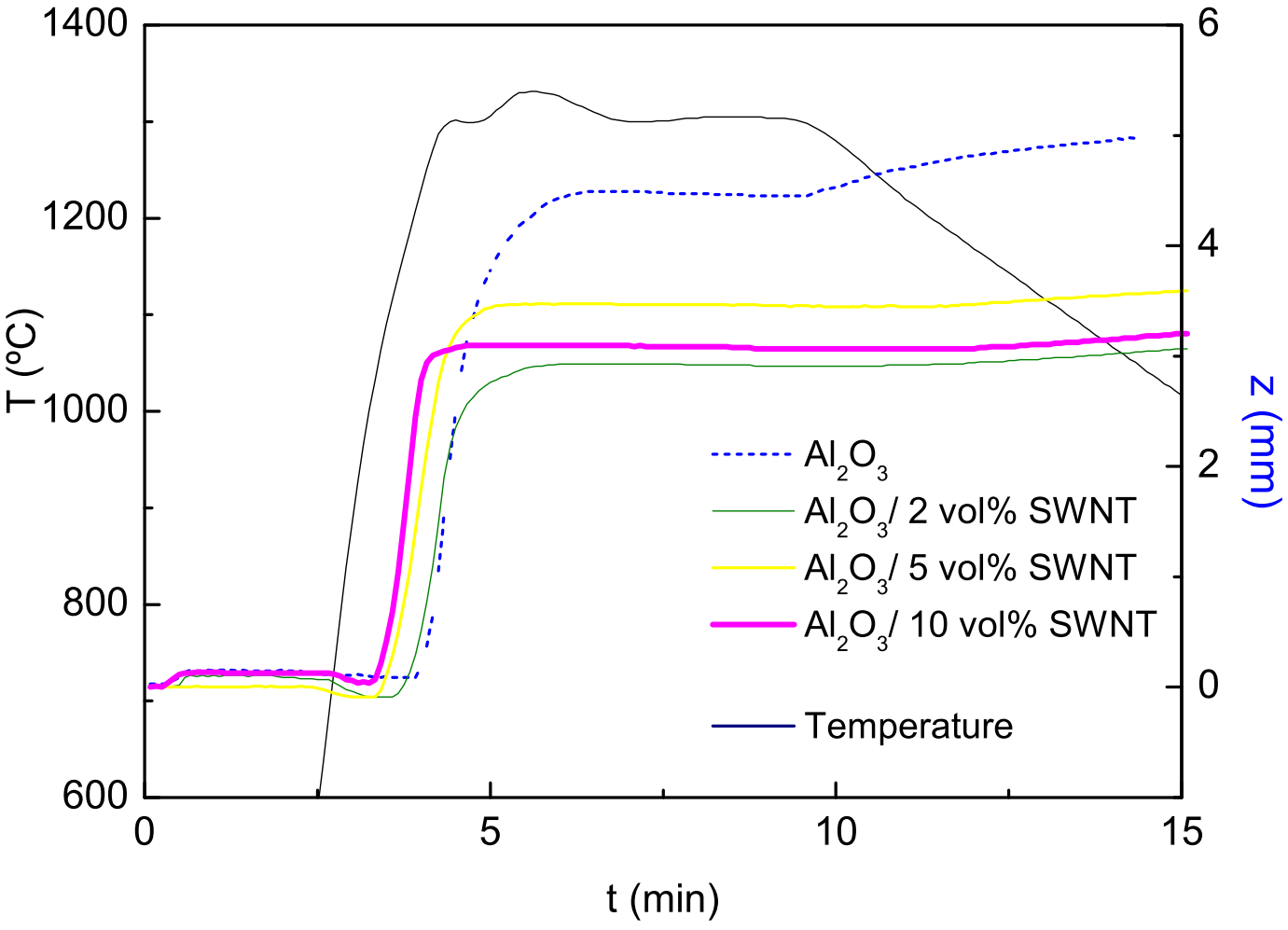

Figure 2
Click here to download Figure: Figura 2 raman.eps

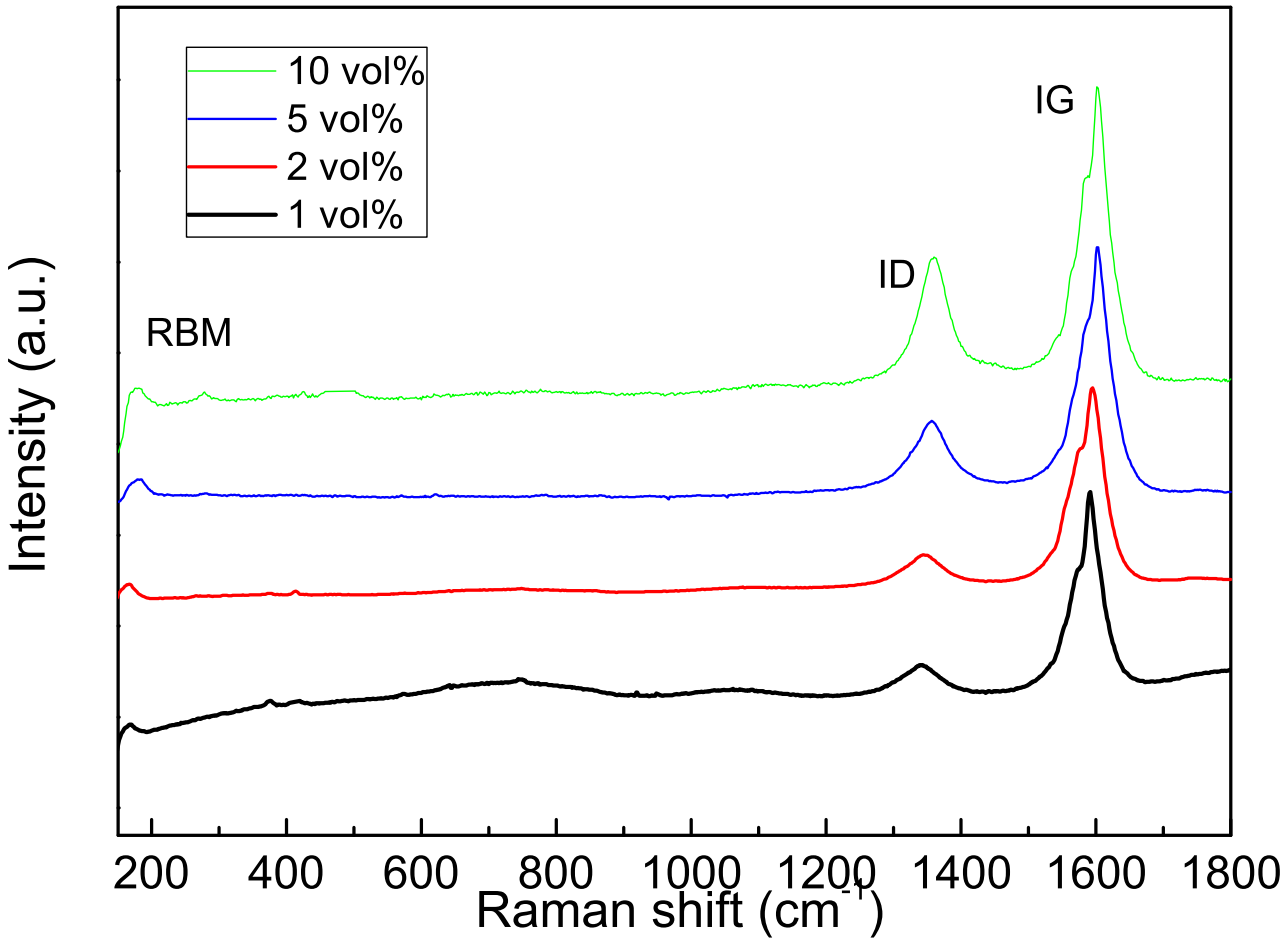

Figure 3
Click here to download Figure: Fig3new.docx

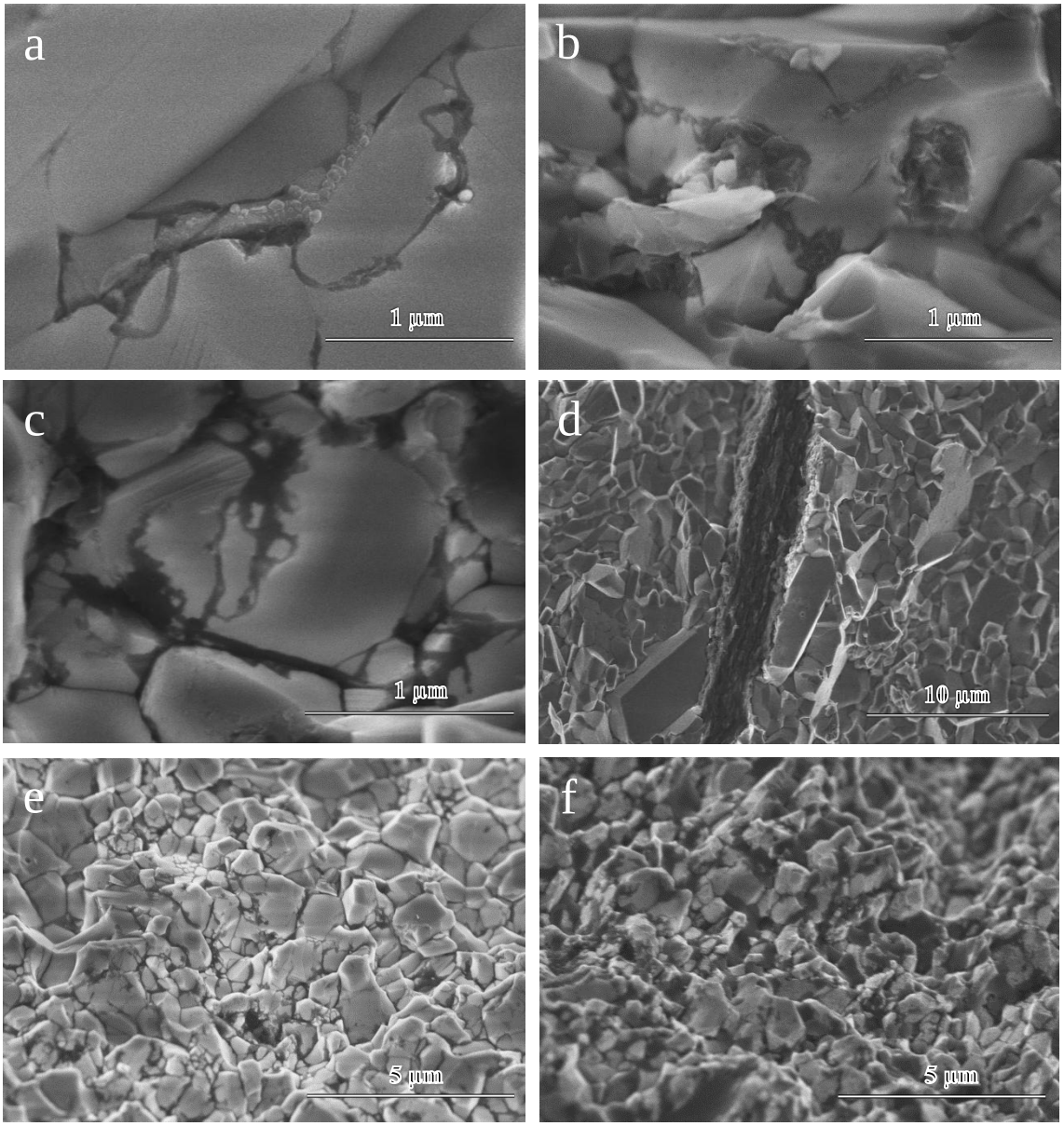

Figure 4
Click here to download Figure: Fig4.docx

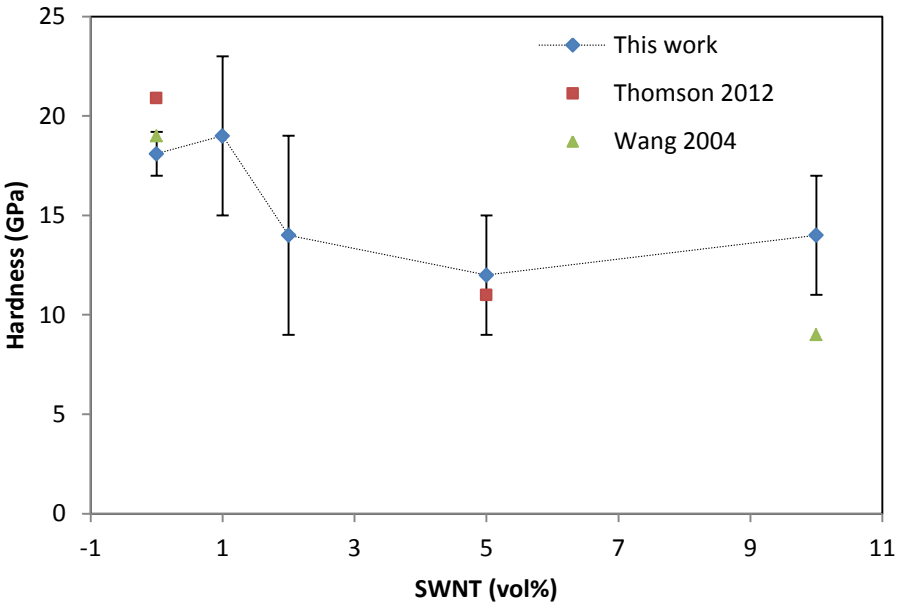

Figure 5
Click here to download Figure: Figura 5.docx

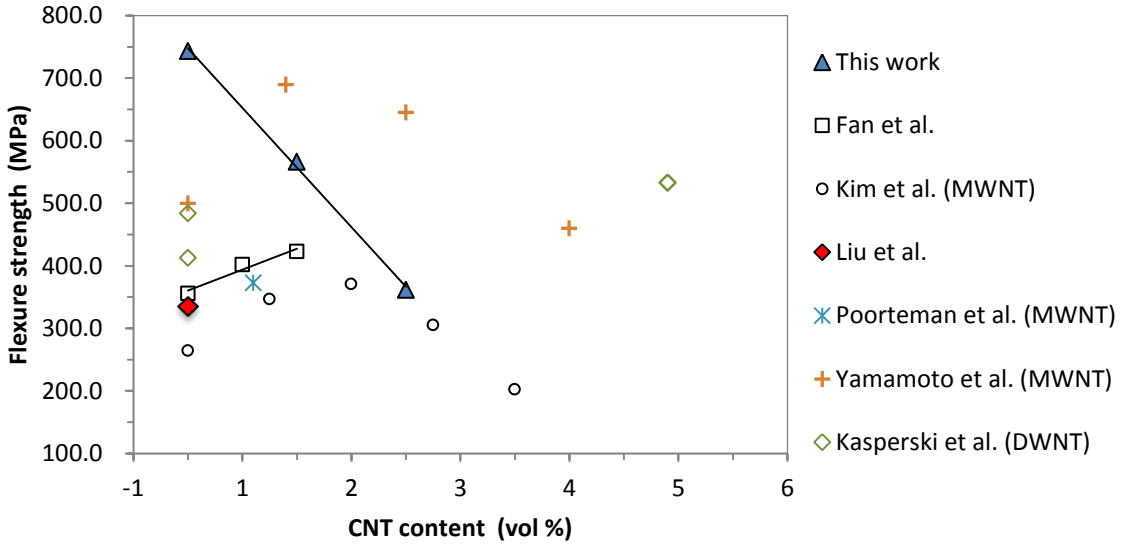

Table 1
Click here to download Table: Table 1 rev.docx

Table 1 Density and microstructural parameters for Al_2O_3 and SWNT/Al_2O_3 composites.

SWNT vol %	**Relative density (%)**	**d (µm)**	**sd (µm)**	**Shape factor, F**	**Preferential orientation [f_p= 0 – 1]**
0	98.4	0.7	0.6	0.67 ± 0.14	0.3
1	98.5	0.6	0.4	0.68 ± 0.10	0.5
2	99.4	0.7	0.4	0.67 ± 0.12	0.4
5	99.8	0.5	0.4	0.71 ± 0.17	0.4
10	100.0	0.5	0.3	0.72 ± 0.16	0.3

Table 2
Click here to download Table: Table2.docx

Table 2. Flexural strength measured for each tested sample and average values.

SWNT (Vol %)	**σ_f (MPa)**	**$<\sigma_f>$ (MPa)**
0	770 ± 9	740 ± 50
	740 ± 8	
	680 ± 8	
	780 ± 9	
1	570 ± 6	570 ± 50
	610 ± 7	
	520 ± 6	
2	330 ± 4	360 ± 40
	400 ± 4	